Rock Mechanics
and Rock Engineering 22, 1—23 (1989)

**Rock Mechanics
and Rock Engineering**

Measurement of Rock Mass Deformation with Grouted Coaxial Antenna Cables

By

C. H. Dowding[1], M. B. Su[2], and K. O'Connor[3]

[1] Department of Civil Engineering, Northwestern University, Evanston, IL, U.S.A.
[2] Department of Civil Engineering, National Chung-Hsing University, Taichung, Taiwan, R.O.C.
[3] Department of Mining and Geological Engineering, New Mexico Institute of Mining and Technology, Socorro, NM, U.S.A.

Summary

Techniques presented herein show how reflected voltage pulses from coaxial antenna cable grouted in rock masses can be employed to quantify the type and magnitude of rock mass deformation. This measurement is similar to that obtained from a combined full profile extensometer (to measure local extension) and inclinometer (to measure local shearing). Rock mass movements deform the grouted cable, which locally changes cable capacitance and thereby the reflected wave form of the voltage pulse. Thus, by monitoring changes in these reflection signatures, it is possible to monitor rock mass deformation.

This paper presents laboratory measurements necessary to quantitatively interpret the reflected voltage signatures. Cables were sheared and extended to correlate measured cable deformation with reflected voltage signals. Laboratory testing included development of grout mixtures with optimum properties for field installation and performance of a TDR (Time Domain Reflectometry) monitoring system. Finally, the interpretive techniques developed through laboratory measurements were applied to previously collected field data to extract hitherto unrealized information.

Introduction

The Time Domain Reflectometry (TDR) approach employed in this study was developed initially as a method to locate discontinuities in coaxial transmission cables (Moffitt, 1964). The concept has been extended to measurement of the properties of materials in which coaxial cables are embedded, such as water content of soil (Topp, Davis, and Annan, 1980) and the evaluation of coaxial cable dielectric behavior (Cole, 1975). In rock mechanics specifically, the technique has been

employed to identify zones of rock mass deformation (Panek and Tesch, 1981, and O'Connor and Dowding, 1984) corresponding to locations of cable failure.

The system is quite economical because of the ease of installation, use of commercially available instruments and cable, and the ease of data acquisition and interpretation (Dowding et al., 1986). The coaxial cable

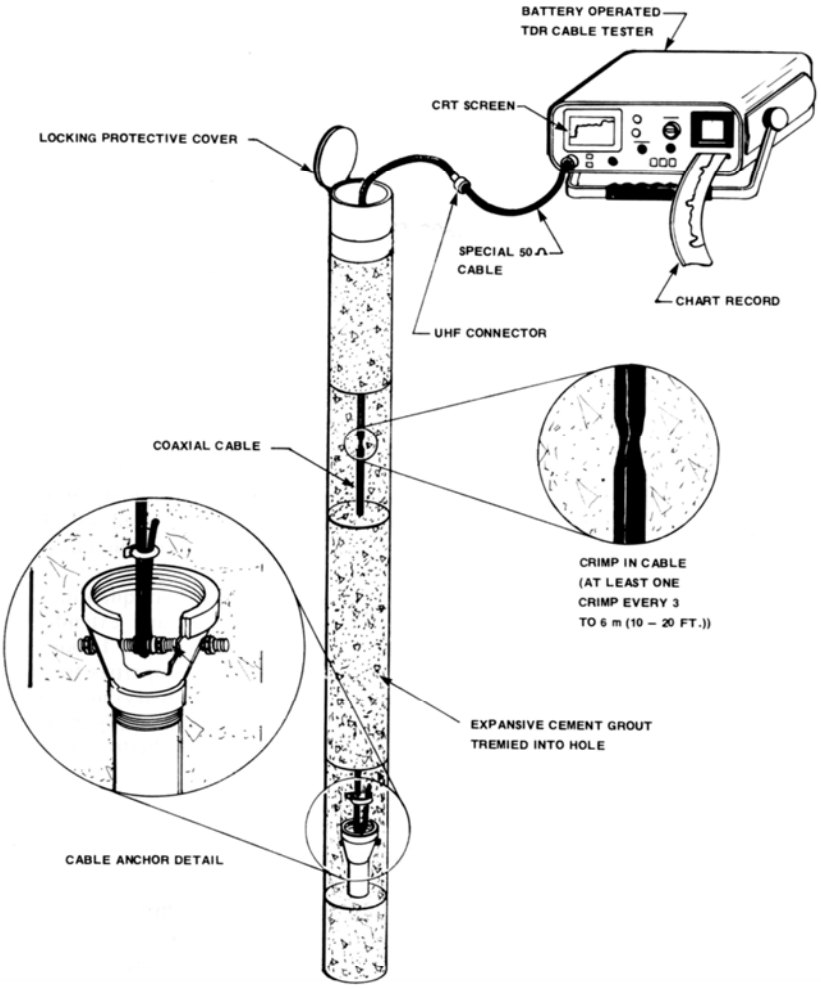

Fig. 1. Features of TDR installation showing relationship between cable and instrumentation (after Dowing and O'Connor, 1984)

(a) TEKTRONIX 1502 TDR CABLE TESTER

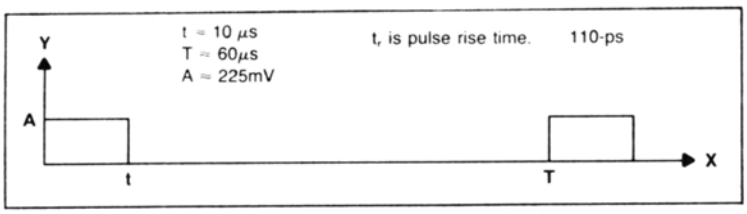

(b) NOMINAL TIME DOMAIN WAVEFORM

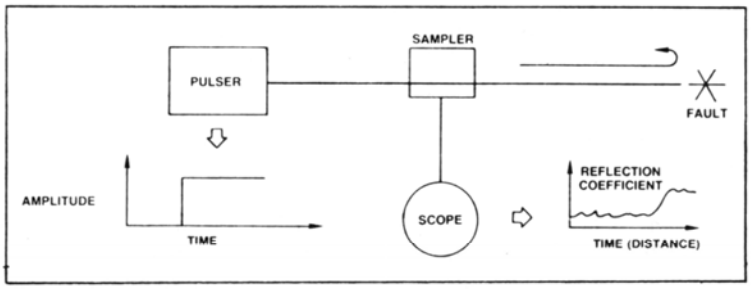

(c) OPERATING PRINCIPLE

Fig. 2. TDR cable tester, time domain waveform and operating principle

costs about $ 1.00 (1986 U. S.) per foot and can be grouted in place with a conventional drilling rig water pump. One portable readout unit (weighing less than 5 lbs) can be employed for monitoring as many cables as desired and produces either a permanent strip chart record or an analog voltage output. These units are mass-produced for other industries and therefore reasonably priced as well as available on a rental basis. The reflected signatures can be interpreted directly from the strip chart record or the analog output can be digitized for automated interpretation. Furthermore, the system is capable of being remotely monitored for critical installations such as sinkhole or coal field subsidence (O'Connor and Dowding, 1984) or underground nuclear tests (Schmitt and Dick, 1985).

Features of a TDR coaxial cable installation are shown schematically in Fig. 1. The bottom of the cable is sealed to prevent water intrusion into the dielectric and is attached to a weighted anchor. As the cable is lowered into the borehole, it is crimped at the desired intervals to provide reference reflections along the cable and bonded to the surrounding rock with an expansive cement grout that is tremied into the hole. A UHF connector is attached to the top-of-hole end and, when making measurements, the cable is connected to Tektronix 1502 TDR cable tester (a photograph of which is shown in Fig. 2a) via a special calibrated 50-ohm cable with a BNC adaptor to provide the reference impedance. The battery-powered TDR cable tester incorporates a video display with a strip chart recorder to provide a permanent record of the video display.

Electrical Property Changes During Cable Deformity

Although the application of TDR for locating and identifying cable faults is not new, quantification of cable deformation has not yet been accomplished. The result of research described in this paper allows such quantification by relating cable deformation to local changes in cable impedance. When a step voltage pulse is transmitted along a coaxial cable, any local changes in cable impedance will cause a partial reflection of voltage at points where the changes exist. Pulse reflections from all changes in impedance along the cable are superimposed on the input pulse to form a series of reflected TDR signatures. Consequently, the composite signature observed on a TDR cable tester screen consists of many individual reflections generated by localized deformations along the cable. The displayed amplitude of the reflection pulses is a function of cable tester settings and is usually calibrated in milli-rhos ($m\rho$) per division for a 50-ohm system.

The time delay (T-t in Fig. 2b) between a transmitted pulse and the reflection from a cable deformity (i. e., cable fault) uniquely determines the fault location. Furthermore, the time, sign, and length and amplitude of the individual reflection pulses define the location, type, and severity respectively of every cable deformity. Figure 2a shows a commercial TDR cable tester that transmits the step voltage pulses and superimposes returned

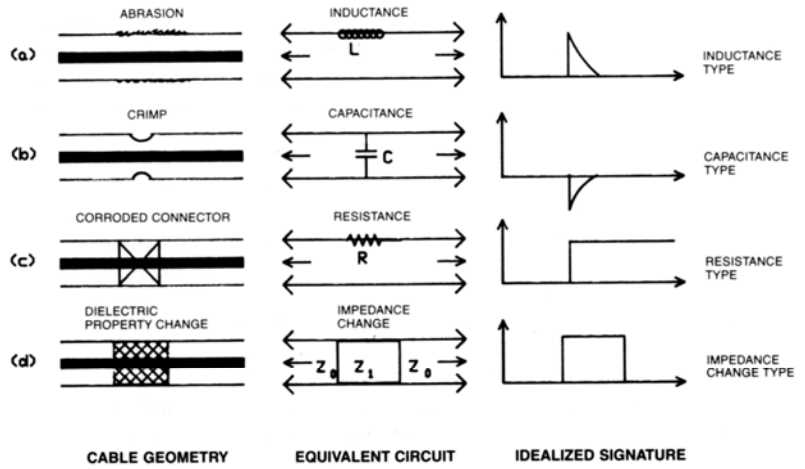

Fig. 3. Idealized TDR cable deformities, associated idealized lumped circuit models, and resulting voltage reflection signatures (after Tektronix, 1983)

voltage pulses on the transmitted voltage pulse. The resultant "reflection coefficient" versus travel time is displayed on the CRT screen.

Figure 3 shows idealized TDR reflection coefficient signatures caused by commonly encountered cable deformities. Signatures are shown along with associated cable geometries and equivalent lumped parameter circuits:

(a) cable abrasion or a partial hole in the outer conductor causes the inductance, L, to increase and produces a local positive spike;
(b) cable crimping (reduction in outer diameter) causes the capacitance, C, to increase and produces a local negative spike;
(c) poor splicing, corroded connectors, or a severed cable causes an increase in resistance, R, and produces increased reflected voltage for downline portions of the cable; and
(d) water within the cable causes a reduction in impedance, $Z(=\sqrt{L/C})$, which produces an increased reflected voltage for the affected section.

A much more detailed explanation of the electromagnetic wave propagation theory and development of numerical modeling schemes can be found in Dowding et al. (1988) and Su (1987).

Shearing and Extension of Cable-Grout Systems

The type and magnitude of reflected TDR signatures caused by shearing and extension was investigated in the laboratory for coaxial cables 9.5, 12.7, and 22.2 mm (3/8, 1/2, and 7/8 in.) in diameter with a

solid aluminum outer conductor. All measurements were made with the Tektronix 1502 TDR cable tester. The coaxial cable was grouted into a steel pipe to simulate a borehole. The expansive grout mix selected for laboratory testing is that recommended for field application and will be discussed later.

Although there are numerous types of semi-flexible coaxial cables that can be employed in TDR monitoring systems, the solid aluminum outer conductor type provides specific advantages as discussed in Dowding et al. (1988). The solid outer conductor is recommended to ensure that the location crimps remain. Braided outer conductors have been observed in field installations to creep with time. The cable should have a large enough diameter to deform a reasonable amount before shearing, yet small (and thus flexible) enough to allow installation without special equipment. A 12.7 mm (1/2 in.) diameter cable optimizes these two requirements. Most importantly, the cable should be installed without the usual outer plastic insulator to ensure a direct grout bond with the outer conductor.

For shearing, the grout and pipe (but not the cable) were cut twice to produce three segments, as shown in Fig. 4, after the grout had cured for 14 days. Each segment represents a rock block while the transverse cuts simulate joint planes. As shown in Fig. 4, the grout and the embedded cable were sheared by pushing the middle segment downward while restraining the two end segments. During the test, relative movement between pipe segments and the associated TDR reflection signature were

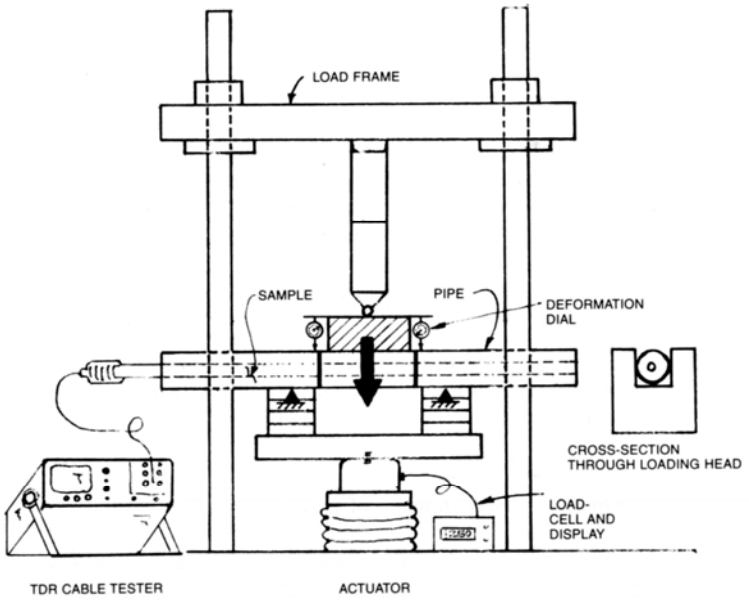

Fig. 4. Apparatus for cable shearing

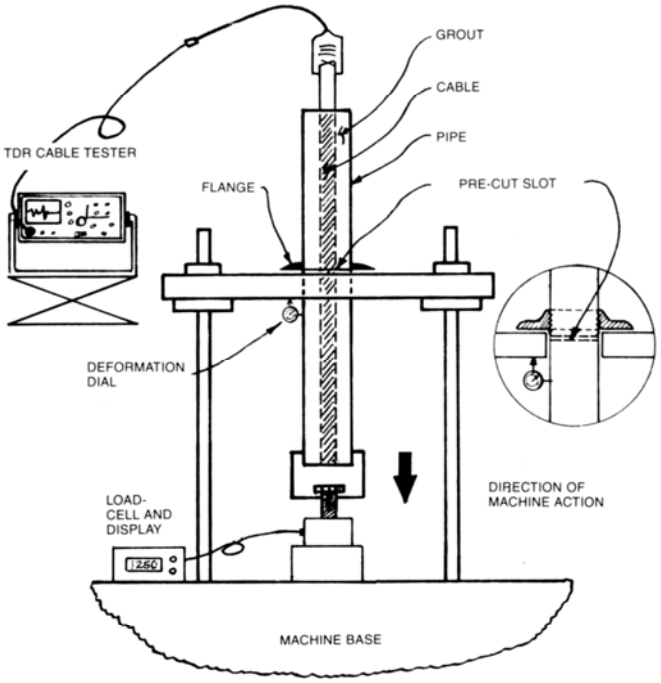

Fig. 5. Apparatus for cable extension

recorded in a digitized form with an analog-to-digital converter in conjunction with an IBM PC/XT.

For extension, the cable was grouted into a steel pipe and cut into two segments after 14 days. As shown in Fig. 5, the grout, pipe, and embedded cable were extended by pulling apart the two pipe segments. The steel pipe transmitted the deformation to the grout which in turn deformed the cable until it either broke in tension or the bond between the cable and grout failed. During the test, the tensile force, relative movement between pipe segments, and the associated TDR reflection signature were recorded in digitized form as done for shearing.

Shear Reflections

Typical load-deformation behavior during shear is presented in Fig. 6 where the arrows correspond with failure of the outer conductor (as indicated by changes in the TDR signature). The initial load-deformation behavior is relatively stiff until failure of the grout at the saw cuts. The irregularity of the subsequent load-deformation behavior is associated with the complex interaction between the grout and coaxial cable with the two shear

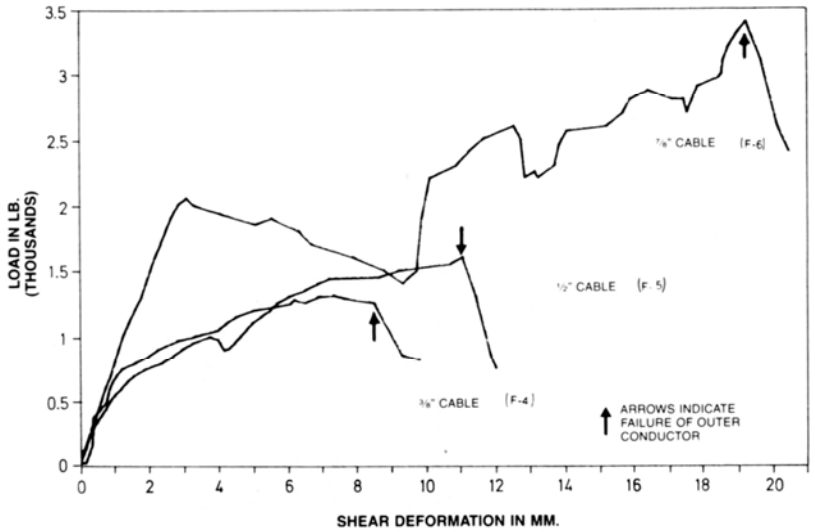

Fig. 6. Relation between shear load and deformation for different sizes of cable showing failure determined by TDR signal interpretation (1 lb = 4.45 N) (1 in. = 25.4 mm)

zones. For the three tests shown in Fig. 6, the shear failure of the cable's outer conductor occurred at deformations of 80% to 90% of the cable diameter under loads of 5782, 6672, and 15123 N (1300, 1500, and 3400 lbs.) for the 9.5, 12.7, and 22.2 mm diameter cables respectively. The cable continued to resist load after failure of the outer conductor because the polyethylene dielectric and inner solid aluminum conductor remained intact.

The change in TDR signature during shear is illustrated in Fig. 7, where it can be seen that the magnitude of the negative reflection coefficient spike increased as the shearing increased. Eventual failure of the outer conductor formed an open circuit and the resultant positive reflection coefficient was shown in the signature corresponding with the 1350 lb load. As indicated by the compilation of test results in Fig. 8, the magnitude of the negative reflection coefficient spike increased linearly with shear deformation but not until an initial deformation had taken place. This initial deformation necessary to generate a detectable reflection appears to depend on the cable diameter, the TDR cable tester settings, and the distance from the cable tester to the shearing location. For cable tester settings of 50 mρ/division (vertical scale) and 0.5 ft/division (horizontal scale), the initial deformation required was 1.58, 1.37, and 7.76 mm (0.063, 0.054, and 0.31 in.) for the 9.5, 12.7, and 22.2 mm diameter cables respectively when shear occurred at a distance of 1.9 m (4 ft) from the cable tester.

A linear best fit of the reflection coefficient vs. shearing relationship in Fig. 8 implies that the sensitivity of the reflection coefficient to cable shear-

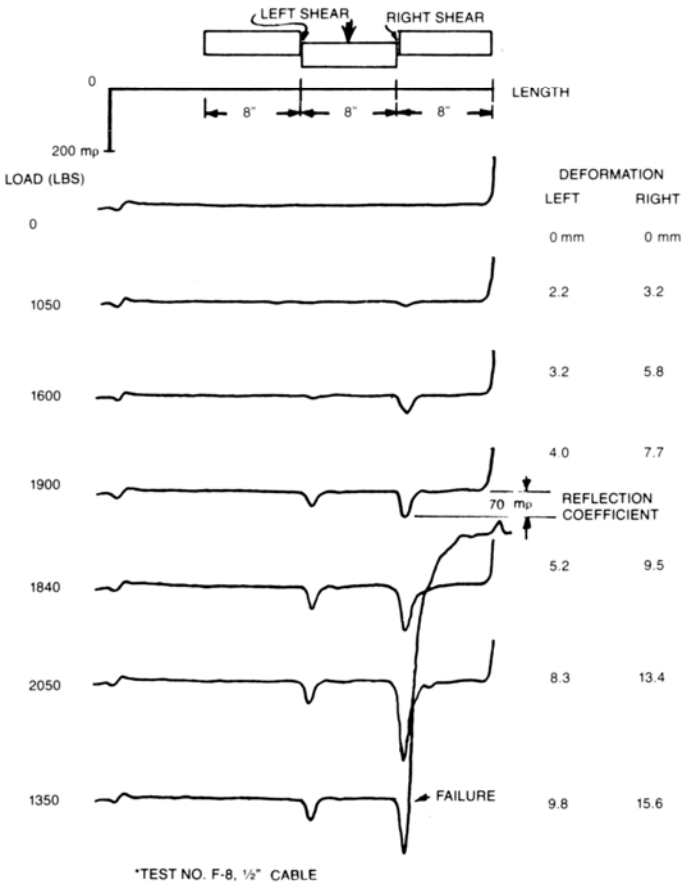

Fig. 7. Reflected voltage signals from shearing 12.7 mm (1/2 in.) cable to failure (1 lb = 4.45 N) (1 in. = 25.4 mm)

ing is 19.99, 33.51, and 17.34 mρ/mm for the 9.5, 12.7, and 22.2 mm diameter cables for the specific laboratory test conditions. To completely generalize these results it will be necessary to perform tests with other TDR cable tester settings and at greater distances along the cable. The smaller diameter cables are more sentitive to shearing, while the larger diameter cables are able to withstand larger range of shear deformation before failure, so a trade-off must be made between sensitivity and range when choosing the coaxial cable to be used for monitoring. In a recent field installation, 12.7 mm diameter cables have been installed in boreholes above a room-and-pillar retreat mine in conjunction with multiple-point extensometers to obtain field verification of the laboratory test results. The

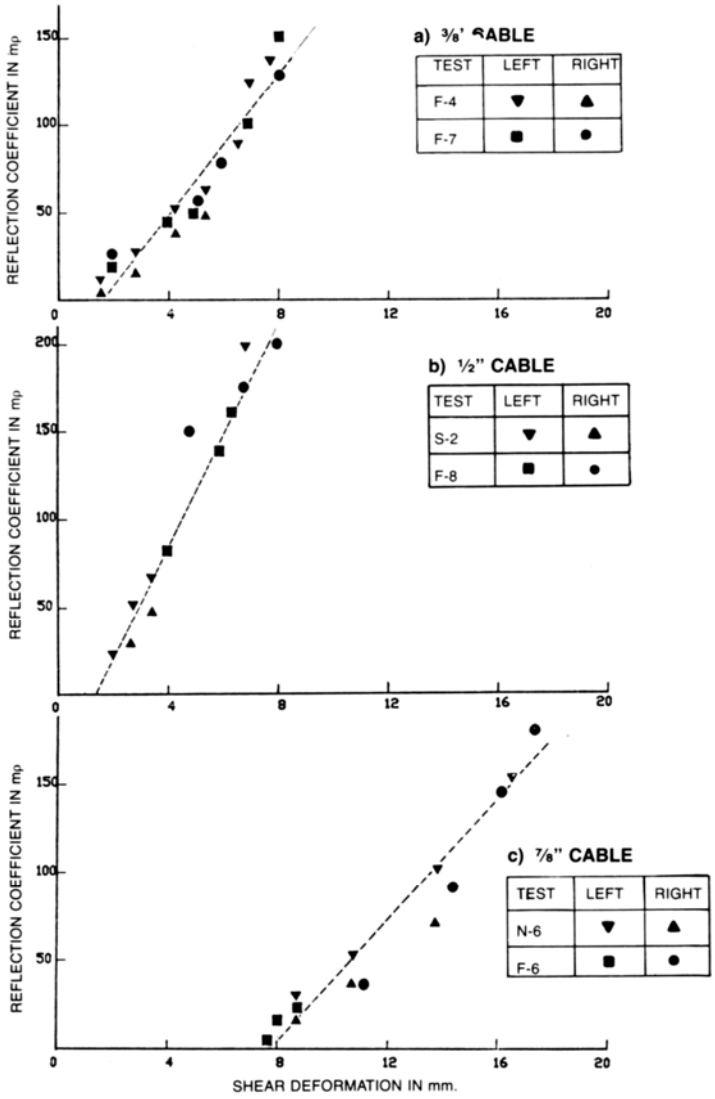

Fig. 8. Relation between reflection coefficient and shear deformation for different sizes of cable (3/8″ = 9.5 mm, 1/2″ = 12.7 mm, 1/8″ = 22.2 mm)

data from this field study are not yet available since mining of the panel has not been started; however, interpretation of existing field data is presented at the end of this paper.

Extension Reflections

Typical extension test results are presented in Fig. 9, where arrows once again correspond with failure of the outer conductor (as indicated by changes in the TDR signature). Similar to the behavior observed during shear, the initial load-deformation behavior in tension is relatively stiff until yielding of the grout at the saw cut. The yield load is proportional to the cable diameter since it was controlled by failure of the grout-cable bond. The yield stress is consistent with a grout-cable bond strength of 270 KN/m^2 (30 psi) assuming an effective bond length of 0.5 m (18 in.). Grout-cable bond strength was determined by performing pull-out tests, as discussed in the Appendix.

While shearing causes a localized deformation of the outer conductor of the coaxial cable, extension causes a necking down of the outer conductor over a greater length of cable than shearing. As shown in Fig. 10, the signature generated by extension is much broader than that shown in Fig. 7 for shear deformation. The length of the signature increases as the cable is extended until either the outer conductor fails or the bond between grout and cable fails (i. e., pull-out occurs). Failure of the outer conductor is indicated in Fig. 10 by an open-circuit condition (large positive reflection coefficient) at the breaking point.

For the tests that were performed, a broad negative TDR signature developed only for the 12.7 mm cable. Neither the 9.5 mm nor the 22.2 mm cable produced a reflection coefficient before cable failure. This unex-

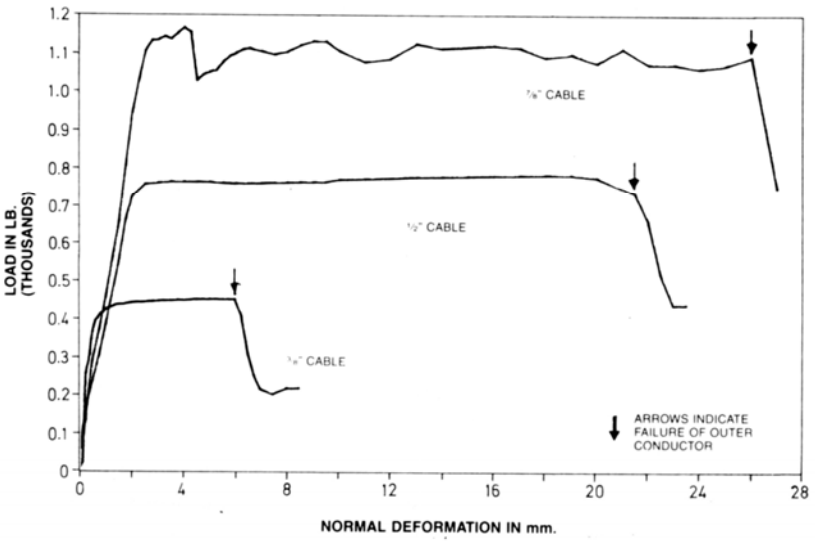

Fig. 9. Relation between normal load and deformation for different sizes of cable showing failure determined by TDR signal interpretation (1 lb = 4.45 N) (1 in. = 25.4 mm)

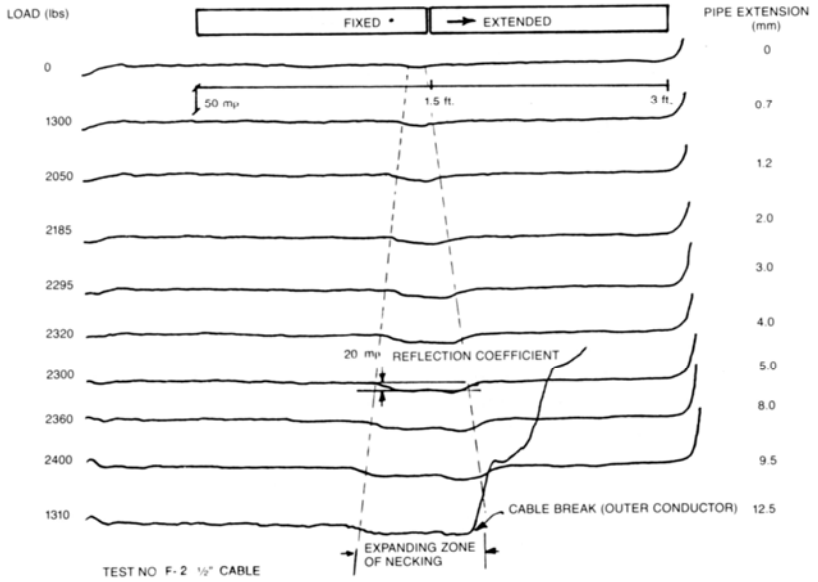

Fig. 10. Reflected voltage signals of 12.7 mm (1/2 in.) cable extended to failure (1 lb = 4.45 N) (1 in. = 25.4 mm)

plainable absence requires further study. For the 12.7 mm cable tested, extension produced a negative reflection coefficient of approximately 20 mρ at failure, as shown by the signature at 2300 lbs in Fig. 10. By comparison, a reflection coefficient of 150 mρ was obtained for shear failure at the same distance from the cable tester using identical tester settings. Consequently, a TDR signature generated by shearing is much more easily detected than a signature generated by extension. This places a limitation on the usefulness of TDR for monitoring cable extension as it is deformed by rock mass movement; however, cable failure due to extension can be distinguished from cable failure due to shear, as will be shown below, in the discussion on interpretation of TDR reflections.

Grout Properties for Economical Installation

Grout material tests were conducted to design a sufficiently strong and expansive grout mixture that could be placed with a water pump on a typical drilling rig. It was desired to design a mixture with low viscosity to allow easy pumping without sacrificing strength. At the same time, it was also desired to prevent shrinkage to ensure that the grout will transfer rock deformation to the cable. These properties were quantified through tests for viscosity, grout-cable bond strength, shrinkage, and unconfined compressive strength for various ratios of water, cement, and additive. The

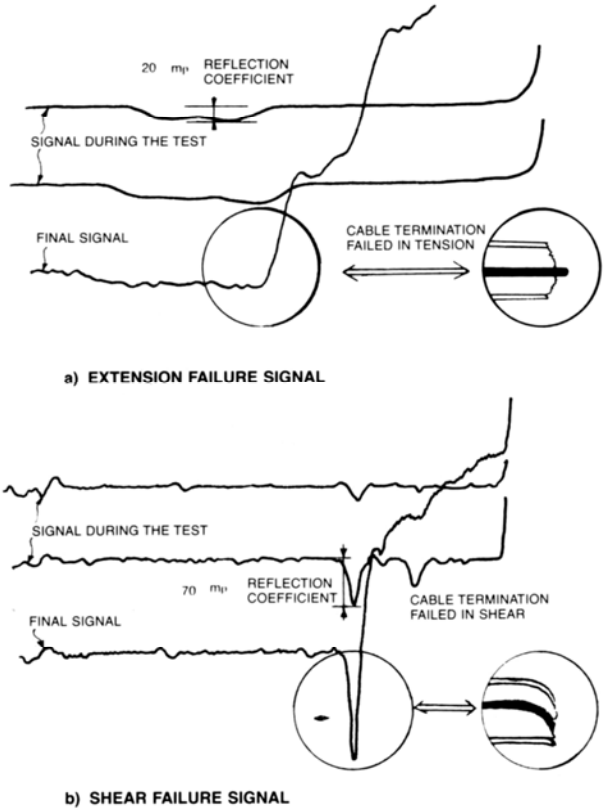

Fig. 11. Comparison of reflected voltage signatures for extension and shear at the failure location showing the large negative spike associated with shearing

cement for the test program was Portland type III, a high early-strength cement, and the additive was Intrusion Aid (Intrusion-Prepakt, 1980). Details of these tests are presented in the Appendix.

Interpretation of Field TDR Reflections

Determination of the type of deformation many times is as imporant as determining the magnitude. Based on laboratory tests, it is now known that shear causes a distinctive voltage reflection spike of short wavelength that increases in direct proportion to shear deformation of the cable. On the other hand, extension causes only a subtle, trough-like voltage reflection that increases in length as the cable is deformed. Obviously, shear deformation causes the more easily detectable reflection.

Although no significant voltage reflection has been observed to develop with progressive cable extension before failure, if the cable is

severed the reflection signature associated with extension failure (severence) differs considerably from the reflection signature associated with that produced by shear failure. As shown in Fig. 11, extension necking produces a small amplitude voltage reflection trough just before the large positive opencircuit reflection (i. e., end of cable at failure). On the other hand, shearing produces a distinctive negative voltage reflection spike just prior to the large positive open-circuit reflection.

Field Measurements

In one application, TDR monitoring cables were installed within the strata overlying two longwall coal mine panels at the Old Ben Mine No. 24 in Benton, Illinois (Wade and Conroy, 1980). The installation consisted of 22.2 mm (0.875 in.) diameter coaxial cable (Cablewave Co., FXA 78-50), which was precrimped and grouted into vertical holes through the overburden stratigraphy shown in Fig. 12b.

TDR traces shown in Fig. 12 were obtained from the monitoring cable installed above the first longwall panel in a position similar to Borehole A in Fig. 12a just prior to undermining of the drillhole location. Consequently, reflection signatures developed as a result of strata fracturing and caving in response to mining of the coal seam. The initial numerous reflections were caused by crimps that had been made in the cable during installation. Subsequent increases in the magnitude of TDR signatures and shortening of cable length are associated with strata separation and caving. If the cable had been positioned at B, more shear events might have been observed before failure by strata separation as the face moved toward the cable.

The TDR traces shown in Fig. 13 were obtained from the monitoring cable installed over a second longwall panel at the same mine. The installation in this case was located approximately 244 m (800 ft) from the beginning of the panel in a position similar to Borehole B in Fig. 12a, and the beginning of the panel in a position similar to Borehole B in Fig. 12a, and the cable was subjected to rock strata response in front of the advancing longwall. The eight TDR traces in Fig. 13 describe cable deformation recorded over a period of approximately one year with the interpreted end of cable indicated with an arrow for each trace. The distance between cable and face is given for each trace with the convention that distance is positive as the face approached the cable and negative as the face moved past the cable.

The differences in signatures between Figs. 12 and 13 occur for several reasons. Fig. 12 was taken from an article, whereas those in Fig. 13 were taken from original data. Thus signatures in Fig. 12 were already interpreted to exclude the reflections after the cable end. Furthermore, the original signatures, shown in Fig. 13, were preserved at such a scale as to allow more detailed interpretation. Scales of presentation of time histories can affect their interpretation. However, such scales do not affect the physics of the basic principle. For instance, data could be recorded

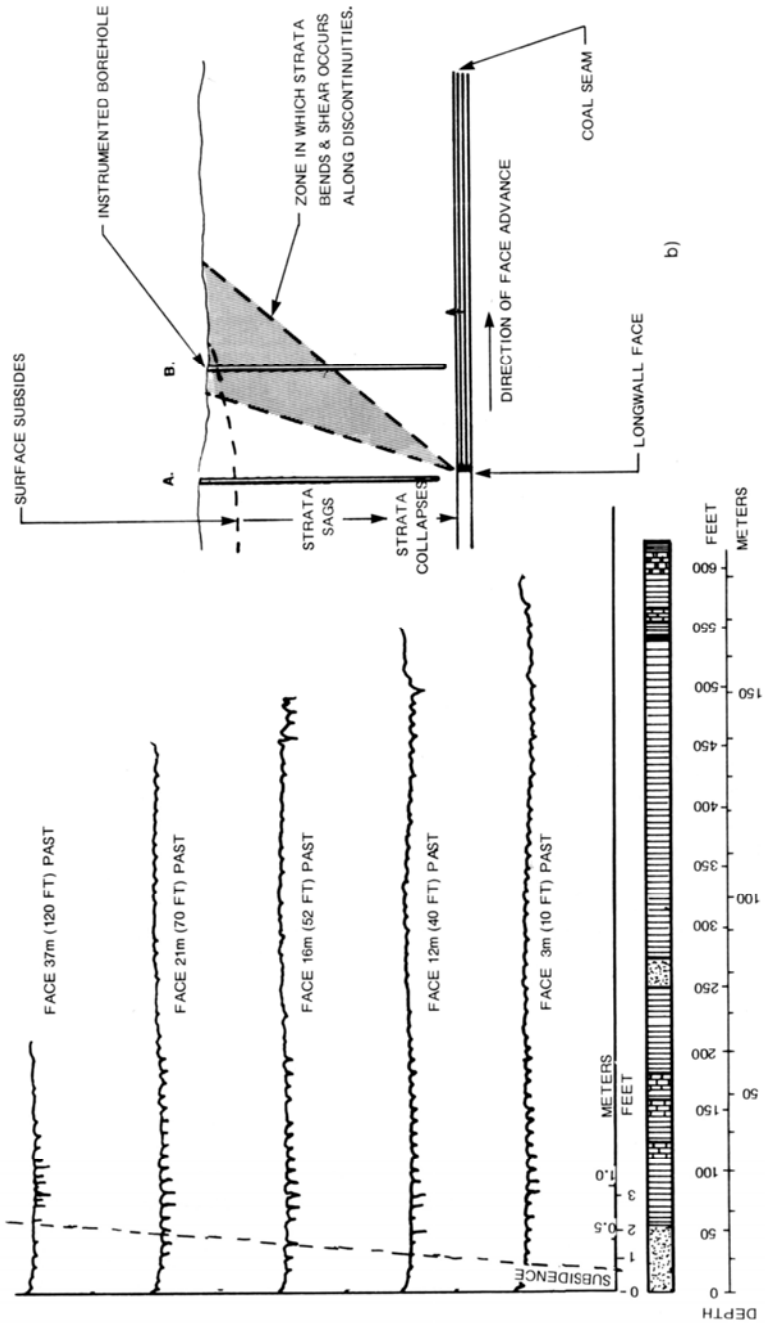

Fig. 12. Strata movement and TDR data for a longwall mine

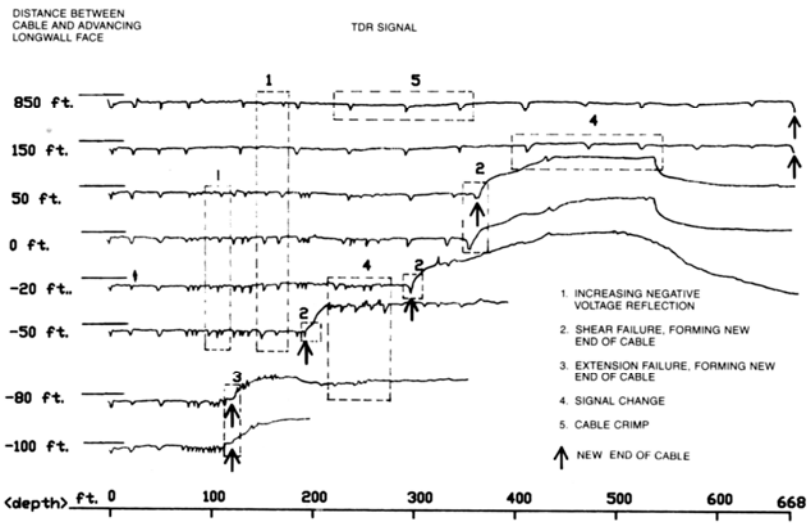

Fig. 13. Interpretation of TDR voltage reflection signatures in a borehole position similar to B in Fig. 12 and produced by collapse of a longwall panel (1 lb = 4.45 N) (1 in. = 25.4 mm)

digitally without depending on the hard copy output of the commercial unit, and subsequently output at any scale desired. In fact, the signatures for the laboratory experiments were recorded in such a fashion.

Increasing local negative reflections, marked as (1) at a depth of 45 m (150 ft), indicate increasing shear deformation of the cable as the face approached. The negative reflection spike (2) on the plot at a depth of 105 m (350 ft) shows that shearing rather than extension severed the cable. On the other hand, tensile failure (3) at a depth of 36 m (120 ft) shows only a slight negative reflection before the large positive open-circuit reflection. Signal changes (4) at a depth of 122 m (400 ft) show locations of secondary or even higher order reflections and do not present new data. Cable crimps (5) made at known distances during installation serve as references for distance along the cable. It will now be shown how to quantify this interpretation based on the relationships presented earlier in this paper.

Example Rate Calculations

Shear discontinuities from Fig. 13 are enlarged for analysis in Fig. 14. These are taken from the reflection traces between the depths of 51 m (170 ft) and 66 m (220 ft) corresponding to the case when the longwall face was 15 m (50 ft) away from the cable and the case when the face was located underneath the cable. Reflection coefficient spikes at 56.3 and 62.8 m (185 and 206 ft) increased from 10 and 13 mρ to 21 and 19 mρ. By referring to the best fit line for laboratory data presented in Fig. 9 for the

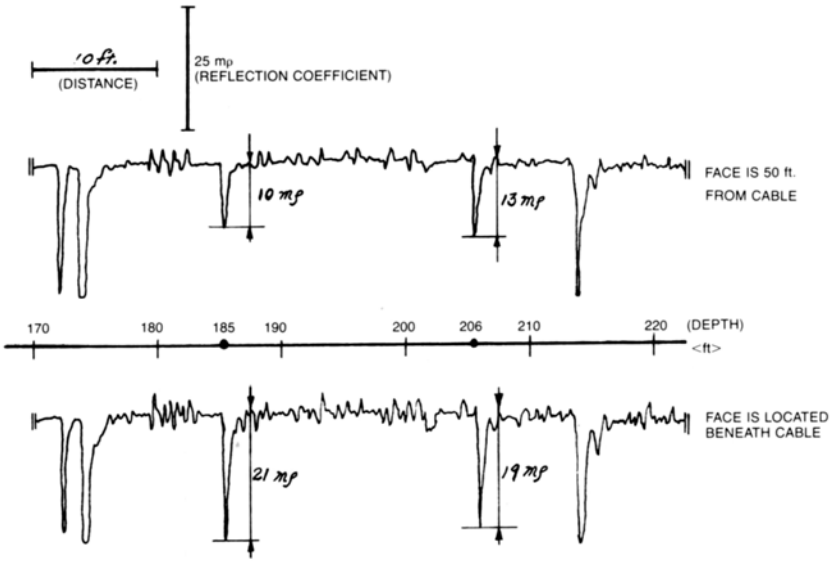

Fig. 14. Detailed interpretation of TDR voltage reflection signatures of Fig. 13 showing change with excavation of longwall panel (1 lb = 4.45 N) (1 in. = 25.4 mm)

22.2 mm cable under shear deformation, shear deformations of 8.3 and 8.5 mm when the face was 15 m (50 ft) away had increased to 9.0 and 8.9 mm respectively by the time the cable was being undermined.

Even though the maximum reflection coefficient on Fig. 14 is 20 mρ, laboratory data indicates that a reflection coefficient of 150 mρ will develop before failure. Unfortunately, the reflection coefficient scale (5 mρ/div) employed during data acquisition did not allow recording of the much greater reflection coefficients that probably occurred before failure. This scale allowed only 10 to 20% of the maximum possible shear information to be recorded (i. e., 80 to 90% of the signature was beyond the limits of the strip chart paper). Consequently, readings should be made at a variety of scales to maximize both sensitivity and range.

Conclusions and Recommendations

Relationships between Time Domain Reflectometry (TDR) reflected voltage signatures and cable deformation have been presented. The formation of the TDR reflection coefficient's signature has been illustrated and a method to quantitatively interpret TDR signatures in terms of cable deformation has been provided. Furthermore, grout and grout-cable interaction properties have been determined and grout mix design recommendations have been provided for cable grouting with typical drilling

equipment. Finally, the interpretive methods which have been developed and reported herein were applied to existing field data to obtain estimates of the magnitude and characteristics of rock mass movements. Based upon these measurements and interpretations the following conclusions are tentatively advanced:

1) Shear deformation of the TDR cable causes an easily detectable TDR reflection spike of short wavelength that increases in magnitude in direct proportion to shear deformation of the cable. Consequently, it is possible to monitor the rate of shear deformation by obtaining a series of TDR records over a period of time.
2) Extension deformation of the TDR cable causes only a subtle, trough-like TDR reflection that increases in length as the cable is deformed. However, cable failure due to extension can be distinguished from that due to shearing by the absence of a shear reflection spike at the point of failure.
3) Based on the mechanical and electrical properties of coaxial cables, a 12.7 mm (1/2 in.) diameter coaxial cable, with a copper clad, aluminum center conductor, low-loss, cellular, polyethylene dielectric; and smooth wall, aluminum outer conductor is recommended. The cable should be installed without the outer insulating jacket in order to maximize bonding with the grout.
4) In order for the grout to act as a backfill material and transmit rock deformation to the cable, it is suggested that the mix design involve a high early-strength cement, a high water-to-cement ratio, and a 2% (by weight) expansive agent. This grout appears to provide adequate bond strength while being fluid enough to be placed with the water pump of a typical drilling rig.
5) Smaller diameter cables are the most sensitive to shearing, while the larger diameter cables are able to withstand larger shear deformation before failure. Measurements on short cables show that the initial deformation necessary to cause a detectable reflection coefficient increases with the cable diameter.
6) Because of the relatively early stage of quantitative interpretation of TDR reflection signatures, further laboratory and field testing, especially with long (60 m; 200 ft) cables, is required to verify the above conclusions.

Acknowledgements

This research was funded by the Office of Surface Mining (OSM) of the U.S. Department of the Interior (DOI) in conjunction with the Illinois Abandoned Mine Lands Reclamation Council. Simultaneous field work is being conducted by the Illinois State Geologic Survey (ISGS). The cooperation of Peter Michael and Robert Bauer of OSM and ISGS has been an important factor in the progress of this project. Records of previous TDR

signatures from longwall mine collapse were provided by Dames and Moore and Peter Conroy of Harza Engineering Co., whose work was sponsored by the U.S. Bureau of Mines also of the U.S. DOI. TDR signatures were recorded with a system on loan from Tektronix. The support and cooperation of these agencies and companies has been instrumental in the conduct of this research and is greatly appreciated.

Appendix

Grout Properties for Economical Installation

Grout material tests were conducted to design a sufficiently strong and expansive grout mixture that could be placed with a typical drilling rig water pump. It was desired to design a mixture with low viscosity to allow easy pumping without sacrificing strength. At the same time, it was also desired to prevent shrinkage to ensure that the grout will transfer rock deformation to the cable. These properties were quantified through tests for viscosity, grout-cable bond strength, shrinkage, and unconfined compressive strength for various ratios of water, cement, and additive. The cement for the test program was Portland type III, a high early-strength cement, and the additive was Intrusion Aid (Intrusion-Prepakt, 1980). Details of these tests are presented below.

Viscosity

Viscosity was determined with a Brookfield Viscometer by measuring the force required to rotate a spindle in the grout at a given angular velocity. The fundamental unit of viscosity is a poise; a material requiring a shear stress of one dyne per square centimeter to produce a rate of shear of one radian per second has a viscosity of one poise or 100 centipoise (cps). The test results presented in Fig. A-1 were obtained at a shear rate of 20 RPM, and all the viscosity tests were performed 10 to 20 minutes after mixing.

In Fig. A-1a viscosity is plotted as a function of water content (i. e., water-to-cement ratio by weight). All samples were prepared with 2% (by weight) of Intrusion Aid (Intrusion-Prepakt Inc., 1980) expansive agent. Increasing the water content from 40 to 60% significantly decreased the viscosity but increasing the water content beyond 60% had little effect as shown by the comparison with 80% water content and no additive. To evaluate the influence of the percent by weight of additive, samples were prepared at a water content of 65% (7.6 gal. of water/94 lb. sack of cement). Comparison with the 80% water content mixture without additive in Fig. A-1b shows that 1% (by weight) additive is as effective as 2% for a water content of 65%.

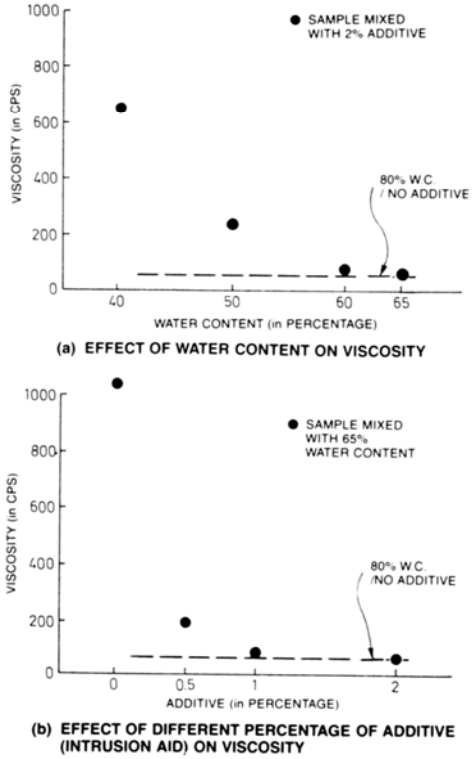

Fig. A-1. Variation of grout viscosity with variation in water to cement ratio (water content) and expansive agent

Paste mixed at 80% water content without additive had a viscosity of 60 cps, which compares well with the data presented by Clarke (1984) for ordinary Portland cement mixed with 100% water content whose viscosity was 50 cps. Grout which has a viscosity of 50 to 60 cps can be placed easily with a conventional drilling rig water pump. More importantly, observations made during a field installation show that grout mixed at 40% water content with 2% additive can be pumped without problem as long as pumps are immediately cleaned. This field mixture would have a viscosity on the order of 600 cps by interpolation of data presented in Fig. A-1a.

Strength and Volume Change of Grout

Strength and volume change properties of the grout must be such that an adequate bond develops between the grout and cable and between the grout and borehole wall. Therefore the unconfined compressive strength, bond strength and volume change characteristics were determined for a

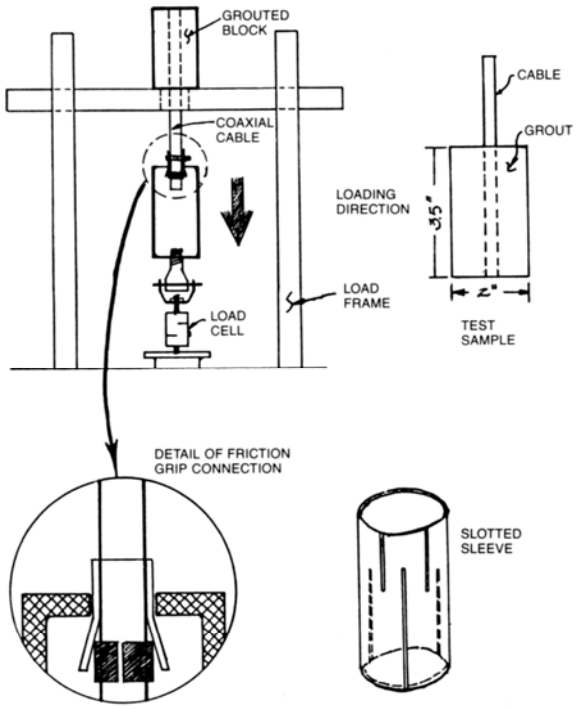

Fig. A-2. Details of the grout pull-out test for unsheathed aluminum cable

variety of grouts. The unconfined compressive strength tests were performed on samples 50.4 mm (2 in.) in diameter and 87.5 mm (3.5 in.) long after curing for 14 days.

The bond strength between the grout and the unsheathed aluminum outer conductor cable was determined by performing pull-out tests as shown in Fig. A-2. A section of cable 152.4 mm (6 in.) long, with a diameter of 12.76 mm (0.5 in.) was grouted into a mold 87.5 mm (3.5 in.) long with an inside diameter of 50.4 mm (2 in.) and allowed to cure for 14 days. The sample was inverted, fixed to the machine frame and a tensile force was applied through the friction grip as shown. Pull-out strength is the maximum load that could be applied to the cable divided by the cable surface area.

Shrinkage or expansion of grout mixtures was determined by measuring the specimen height after curing for 14 days. Because the samples were prepared in stiff rubber molds, free expansion in all directions was possible and the expansion values that were calculated from height changes alone are only to be considered as estimates.

Results of grout stength and volume change tests are summarized in Table A-1, and are consistent with published results. For example, the

Table A-1. *Pumpalbe Grout Properties*

Sample number	Water content	Additive	Compressive strength		Pull-out strength		Volume change
	[wt. %]	[wt. %]	[kN/m²]	[psi]	[kN/m²]	[psi]	[%]
1	65	2	8,480	1,230	209	30.3	−16
2	65	1	8,550	1,240	219	31.7	− 8
3	65	0	1,379	200	269	39.0	−14
4	55	0.5	9,970	1,446	278	40.4	− 3
5	55	0	22,180	3,217	374	54.2	− 3
6	75	0.5	7,467	1,083	209	30.3	−17
7	40	1	12,845	1,863	485	70.3	+ 2
8	50	1	11,342	1,645	446	64.7	+ 1
9	60	1	9.929	1,440	393	57.0	− 2

* (−) volume change is shrinkage
* (+) volume change is expansion

Note: All samples were prepared using Type III high early strength Portland Cement and Intrusion Aid additive.

unconfined compressive strength data presented in Powers (1968) show a 28-day strength of 14,400 kN/m² (1600 psi) for paste mixed with 70% water content. Pull-out strengths presented by Mindess and Young (1981) show the average pull-out stength for a plain steel bar in paste mixed with 80% water content is about 900 kN/m² (100 psi). This value is higher than the results listed in Table A-1, which may be due to the chemical reaction observed between the aluminum outer conductor and high-pH cement paste.

Based on these laboratory test results as well as field observations that grout with water content as low as 40% (and 1% additive) can be placed with a drilling water pump, recommendations can be made for an appropriate grout mix. It appears that water content ratios between 40 and 60% with at least 1% additive will produce a pumpable grout that sets up with adequate strength and no shrinkage. Mixes with 65% water content are acceptable but must be considered as the upper bound for grout water content.

References

Cablewave Systems (1985): Antenna and Transmission Line Systems. Catalog 600, North Haven, Connecticut.

Clarke, W. J. (1984): Performance Characteristics of Microfine Cement. Preprint 84-023, American Society of Civil Engineers, 14 p.

Cole, R. H. (1975): Evaluation of Dielectric Behavior by Time Domain Spectroscopy, 1, Dielectric Response by Real Time Analysis, 2, Complex Permeability, 3, Precision Difference Methods. J. Phys. Chem. *79* (no. 149, 1459—1474).

Conroy, P. (1983): Private Communication, Vice President for Engineering, Harza Engineering Co., Chicago, Illinois.

Dowding, C. H., Su, M. S., O'Connor, K. (1986): Choosing Coaxial Cable for TDR Monitoring. Proceedings of the 2nd Workshop on Surface Subsidence Due to Underground Mining, Morgantown, West Virginia, pp. 153—162.

Dowding, C. H., Su, M. B., O'Connor, K. (1989): Principle of Time Domain Reflectometry Applied to Measurement of Rock Mass Deformation, accepted for publication in the Int. J. Rock Mech. Min. Sci.

Intrusion-Prepakt, Inc. (1980): Intrusion Aid. Cleveland, Ohio.

Mindess, S., Young, J. F. (1981): Concrete. John Wiley & Sons, New York.

Moffitt, L. R. (1964): Time Domain Reflectometry — Theory and Applications. Engineering Design News, November, pp. 38—44.

Mooijweer, H. (1971): Microwave Techniques. McMillan, London.

O'Connor, K. M., Dowding, C. H. (1984): Application of Time Domain Reflectometry to Mining. Proceedings of 25th Symposium on Rock Mechanics, Northwestern University, Evanston, Illinois, pp. 737—746.

Panek, L. A., Tesch, W. J. (1981): Monitoring Ground Movements Near Caving Slopes — Methods and Measurements, RI 8585, U.S. Bureau of Mines, Denver, Colorado, 108 p.

Powers, T. C. (1968): The Properties of Fresh Concrete. John Wiley & Sons, New York.

Schmitt, G. G., Dick, R. D. (1985): Use of CORRTEX (Continuous Reflectometry for Radius and Time Experiments) to Measure Explosive Performance and Stem Behavior in Oil Share Fragmentation Tests. Proceedings of the First Mini-Symposium on Explosives and Blasting Research, Society of Explosives Engineers, Montville, Ohio.

Su, M. B. (1987): Quantification of Cable Deformation with Time Domain Reflectometry Techniques, Ph. D. Dissertation, Northwestern University, Evanston, Illinois.

Tektronix (1983): TDR for Cable Testing, Tektronix Application Note, AX-3241-1, Beaverton, Oregon.

Topp, G. C., Davis, J. C., Annan, A. P. (1980): Electromagnetic Determination of Soil Water Content: Measurements in Coaxial Transmission Lines. Water Resources Research, *16* (no. 3), 574—582.

Wade, L. V., Conroy, P. J. (1980): Rock Mechanics Study of a Longwall Panel. Mining Engineering, December, pp. 1728—1734.

Printed in Austria